A Hybrid Underwater Glider for Underwater Docking

Shilin Peng [1], Canjun Yang [1], Shuangshuang Fan [1], Shaoyong Zhang [1], Pinfu Wang [1], Yu Xie [1], Ying Chen [1, 2]
[1]. The State Key Lab of Fluid Power Transmission and Control, Zhejiang University, Hangzhou, China
[2]. Ocean College, Zhejiang University, Hangzhou, China
pengshilin@zju.edu.cn

***Abstract*—Underwater gliders have the advantage of high endurance and long range. However, these buoyancy-driven gliders do not have horizontal flight capabilities and have the shortage of low maneuverability. In this paper, we present a hybrid underwater glider aiming to overcome these disadvantages. The hybrid glider has characteristics as follows: it combines the capacity of a typical glider and a propeller-driven AUV, having the horizontal fly ability and higher maneuverability; it has the ability to dock with an underwater station for battery recharging and data communication, which will further expand the range and endurance of the vehicle.**

Keywords—hybrid glider; underwater glider; dock; rotatable thruster

I. INTRODUCTION

Underwater gliders are highly efficient, winged underwater vehicles which propel themselves by modulating their buoyancy and attitude[1]. They are widely used in oceanographic research due to their features of low cost, long range and high endurance. The high endurance of gliders is achieved by moving slowly and by keeping down the hotel and sensor load[2]. However, the low-speed capability has significant problems when operating in areas of strong water currents which exceed the glider's maximum forward speed[3]. Moreover, as gliders do not have horizontal flight capabilities, they are limited in certain applications. In contrast, conventional propeller-driven AUVs have higher maneuverability, but their endurance usually ranges from hours to days.

To combined the advantages of this two type of underwater vehicles, a novel type of hybrid glider which combines the features of gliders and AUVs were proposed[4, 5] and several hybrid gliders were developed in previous studies. A. Alvarez fabricated a hybrid glider Folaga[6, 7]; B Claus et al. developed a low-power propeller-based propulsion to augment the buoyancy engine of a 200m Slocum electric glider[3]; S. X. Wang et al. developed a hybrid glider named PETREL[8, 9]. By the hybrid design, these hybrid gliders achieve higher maneuverability while maintaining high endurance. Despite this, if a hybrid glider can dock with an underwater station, we would further enhance the endurance of the vehicle and extend the glider's applications. To this end, a hybrid glider for underwater docking is developed in Zhejiang University. In this paper, we present the design and preliminary testing of this hybrid glider.

II. DESIGN CONSIDERATIONS

For a hybrid glider with docking capability, there are certain constrains placed on the vehicle design. First, the maximum forward speed in AUV mode should exceed 0.7 m/s[3], so that the vehicle can conquer the influence of the current. In our design, the maximum forward speed is design to be 0.9 m/s. Next, to maintain the long endurance of the glider, the efficiency of the thruster should be maximized. In addition, the thruster should have low speed mode to achieve low power consumption. Finally, as the maxim forward speed is less than conventional AUVs, the vehicle should have high maneuverability in low speed to dock with an underwater station.

Conventional AUVs use control fins to control the yaw and pitch. As their steering capability is strongly coupled to their velocity, they have to reach a certain speed before being able to be steered[10]. Since the speed of our glider is not high, the traditional fin-steering method is not fit for our case. In our case, we aim to design a hybrid glider whose yaw is controlled by the rotation of the thruster and whose pitch is control by the longitudinal moving mass. In addition, a lateral moving mass is designed to control the roll and to balance the effect of the propeller torque. By using a rotatable thruster, the vehicle can achieve high maneuverability in low speed.

III. DYNAMIC MODEL

The multi-body dynamic model of the vehicle based on Newton–Euler equations is first derived. The hybrid glider is modeled as a rigid body (mass m_{rb}) with two moving point masses (mass m_{px} and m_{pxy}). The vehicle also includes a variable ballast actuator whose effect is represented by a fixed-position point mass (m_{b}) with variable volume ($\tilde{\mathrm{V}}_{\mathrm{b}}$). The total vehicle mass is:

$$m = m_{\mathrm{rb}} + m_{\mathrm{px}} + m_{pxy} + m_{\mathrm{b}}$$

The vehicle displaces a deformable volume of fluid $\mathrm{V}_{\mathrm{veh}}$ so that the net weight can be described as

$$W = mg - \rho g \mathrm{V}_{\mathrm{veh}} = -\rho g \tilde{\mathrm{V}}_{\mathrm{b}}$$

where ρ is the density of the water and $\tilde{\mathrm{V}}_{\mathrm{b}}$ is the rate of change of varied volume, enabling buoyancy-powered propulsion. If W is greater than zero, the vehicle is heavier

978-0-933957-40-4 ©2013 MTS

than the fluid it displaces and tends to sink, while if W is negative, the vehicle is buoyant and tends to rise.

A. Kinematics

Define a body-fixed, orthonormal reference frame centered at the center of buoyancy of the vehicle and represented by the unit vectors $\boldsymbol{b}_1$, $\boldsymbol{b}_2$, and $\boldsymbol{b}_3$. The vector $\boldsymbol{b}_1$ is aligned with the longitudinal axis of the vehicle, $\boldsymbol{b}_2$ points out the right wing, and $\boldsymbol{b}_3$ completes the right-handed triad(see Fig. 1).

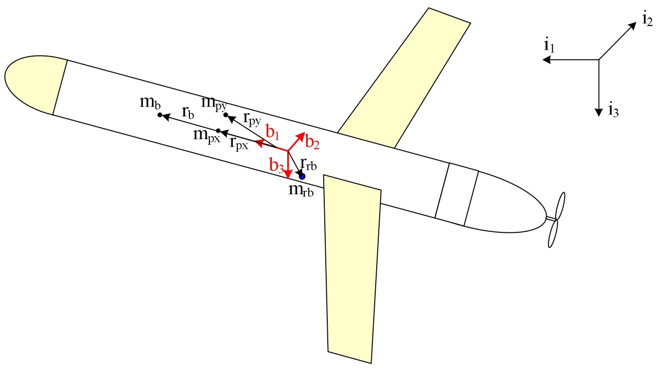

Fig. 1 Illustration of hybrid glider rigid body and mass particles

Define another orthonormal reference frame, denoted by the unit vectors $\boldsymbol{i}_1$, $\boldsymbol{i}_2$, and $\boldsymbol{i}_3$, which is fixed in inertial space such that $\boldsymbol{i}_3$ is aligned with the force due to gravity. The choices of frames are consistent with the underwater vehicle literature, as in [11]. The relative orientation of these two reference frames is given by the proper rotation matrix $\boldsymbol{R}_{\mathrm{IB}}$, which maps free vectors from the body-fixed reference frame into the inertial reference frame[11] Let $\boldsymbol{e}_i$ represent the standard basis vector for $\mathbb{R}^3$, $i \in 1,2,3$, and let the character $\hat{}$ denote the 3×3 skew-symmetric matrix satisfying $\hat{\boldsymbol{a}}\boldsymbol{b} = \boldsymbol{a}\times\boldsymbol{b}$ for vectors $\boldsymbol{a}$ and $\boldsymbol{b}$. Then, in terms of conventional Euler angles (roll angle φ, pitch angle θ, and heading angle ψ), we have

$$\boldsymbol{R}_{\mathrm{IB}}(\varphi,\theta,\psi) = e^{\widehat{\boldsymbol{e}}_3\psi} e^{\widehat{\boldsymbol{e}}_2\theta} e^{\widehat{\boldsymbol{e}}_1\varphi}$$

where $e^{(\cdot)}$ denotes the matrix exponential[12].

Let the inertial vector $\boldsymbol{X} = [X, Y, Z]^T$ represent the position vector from the origin of the inertial frame to the origin of the body frame. Let $\boldsymbol{v} = [u, v, w]^T$ and $\boldsymbol{\omega} = [p, q, r]^T$ represent the translational and rotational velocity of the body with respect to the inertial frame, but expressed in the body frame. The kinematic equations are:

$$\dot{\boldsymbol{X}} = \boldsymbol{R}_{\mathrm{IB}}\boldsymbol{v} \tag{1}$$

$$\dot{\boldsymbol{R}}_{\mathrm{IB}} = \boldsymbol{R}_{\mathrm{IB}}\hat{\boldsymbol{\omega}} \tag{2}$$

In addition to the six degrees of freedom associated with the vehicle's translation and rotation, there are two degrees of freedom associated with the moving masses m_{px} and m_{pxy}, where m_{px} moves along $\boldsymbol{b}_1$ and m_{pxy} moves along $\boldsymbol{b}_2$ while moving together with m_{px} in $\boldsymbol{b}_1$ axis. Let $\boldsymbol{r}_{\mathrm{px}}$ denotes m_{px}'s position with respect to the body frame origin, and $\boldsymbol{r}_{\mathrm{pxy}}$ denotes m_{pxy}'s position with respect to the body frame origin, both expressed in the body frame. As m_{pxy} is a part of pitch moving mass, it moves together with m_{px} (i.e. $\boldsymbol{r}_{px}\cdot\boldsymbol{e}_1 = \boldsymbol{r}_{pxy}\cdot\boldsymbol{e}_1$). The kinematics of the moving mass particles relative to inertial space is

$$\boldsymbol{v}_{\mathrm{px}} = \boldsymbol{v} + \boldsymbol{\omega}\times\boldsymbol{r}_{\mathrm{px}} + \dot{\boldsymbol{r}}_{\mathrm{px}} \tag{3}$$

$$\boldsymbol{v}_{\mathrm{pxy}} = \boldsymbol{v} + \boldsymbol{\omega}\times\boldsymbol{r}_{\mathrm{pxy}} + \dot{\boldsymbol{r}}_{\mathrm{pxy}} \tag{4}$$

B. Dynamics

To derive the equations of motion, we must first determine the kinetic energy of the body/fluid/particle system in order to compute the momenta[13]. We start by defining then kinetic energy of the particles

$$T_{\mathrm{px}} = \frac{1}{2} m_{\mathrm{px}} \boldsymbol{v}_{\mathrm{px}}^T \boldsymbol{v}_{\mathrm{px}} = \frac{1}{2}\boldsymbol{\eta}^T \mathbb{M}_{\mathrm{px}}(\boldsymbol{r}_{\mathrm{px}})\boldsymbol{\eta}$$

$$T_{\mathrm{pxy}} = \frac{1}{2} m_{\mathrm{pxy}} \boldsymbol{v}_{\mathrm{pxy}}^T \boldsymbol{v}_{\mathrm{pxy}} = \frac{1}{2}\boldsymbol{\eta}^T \mathbb{M}_{\mathrm{pxy}}(\boldsymbol{r}_{\mathrm{pxy}})\boldsymbol{\eta}$$

where

$$\boldsymbol{\eta} = \begin{pmatrix} \boldsymbol{v} \\ \boldsymbol{\omega} \\ \dot{\boldsymbol{r}}_{\mathrm{px}} \\ \dot{\boldsymbol{r}}_{\mathrm{pxy}} \end{pmatrix}$$

denotes the generalized velocity of the vehicle,

$$\mathbb{M}_{\mathrm{px}}(\boldsymbol{r}_{\mathrm{px}}) = m_{\mathrm{px}} \begin{pmatrix} \mathbb{I} \\ -\hat{\boldsymbol{r}}_{\mathrm{px}} \\ \mathbb{I} \\ \boldsymbol{0} \end{pmatrix} \begin{pmatrix} \mathbb{I} \\ -\hat{\boldsymbol{r}}_{\mathrm{px}} \\ \mathbb{I} \\ \boldsymbol{0} \end{pmatrix}^T$$

$$= \begin{pmatrix} m_{\mathrm{px}}\mathbb{I} & -m_{\mathrm{px}}\hat{\boldsymbol{r}}_{\mathrm{px}} & m_{\mathrm{px}} & \boldsymbol{0} \\ m_{\mathrm{px}}\hat{\boldsymbol{r}}_{\mathrm{px}} & -m_{\mathrm{px}}\hat{\boldsymbol{r}}_{\mathrm{px}}\hat{\boldsymbol{r}}_{\mathrm{px}} & m_{\mathrm{px}}\hat{\boldsymbol{r}}_{\mathrm{px}} & \boldsymbol{0} \\ m_{\mathrm{px}} & -m_{\mathrm{px}}\hat{\boldsymbol{r}}_{\mathrm{px}} & m_{\mathrm{px}} & \boldsymbol{0} \\ \boldsymbol{0} & \boldsymbol{0} & \boldsymbol{0} & \boldsymbol{0} \end{pmatrix}$$

denotes the generalized inertia matrix for the moving particle m_{px}, and

$$\mathbb{M}_{\mathrm{pxy}}(\boldsymbol{r}_{\mathrm{pxy}}) = m_{\mathrm{pxy}} \begin{pmatrix} \mathbb{I} \\ -\hat{\boldsymbol{r}}_{\mathrm{pxy}} \\ \boldsymbol{0} \\ \mathbb{I} \end{pmatrix} \begin{pmatrix} \mathbb{I} \\ -\hat{\boldsymbol{r}}_{\mathrm{pxy}} \\ \boldsymbol{0} \\ \mathbb{I} \end{pmatrix}^T$$

$$
= \begin{pmatrix} m_{\mathrm{pxy}}\mathbb{I} & -m_{\mathrm{pxy}}\hat{\boldsymbol{r}}_{\mathrm{pxy}} & \mathbf{0} & m_{\mathrm{pxy}} \\ m_{\mathrm{pxy}}\hat{\boldsymbol{r}}_{\mathrm{pxy}} & -m_{\mathrm{pxy}}\hat{\boldsymbol{r}}_{\mathrm{pxy}}\hat{\boldsymbol{r}}_{\mathrm{pxy}} & \mathbf{0} & m_{\mathrm{pxy}}\hat{\boldsymbol{r}}_{\mathrm{pxy}} \\ \mathbf{0} & \mathbf{0} & \mathbf{0} & \mathbf{0} \\ m_{\mathrm{pxy}} & -m_{\mathrm{pxy}}\hat{\boldsymbol{r}}_{\mathrm{pxy}} & \mathbf{0} & m_{\mathrm{pxy}} \end{pmatrix}
$$

denotes the generalized inertia matrix for the moving particle m_{pxy}. Note that throughout the text, $\mathbf{0}$ represents a matrix of zeros whose dimensions will be clear from the context.

The buoyancy control system of the glider is considered as a mass and position-fixed particle. The generalized inertia matrix for the buoyancy control system is

$$
\mathbb{M}_{\mathrm{b}} = \begin{pmatrix} m_{\mathrm{b}}\mathbb{I} & -m_{\mathrm{b}}\hat{\boldsymbol{r}}_{\mathrm{b}} & \mathbf{0} & \mathbf{0} \\ m_{\mathrm{b}}\hat{\boldsymbol{r}}_{\mathrm{b}} & -m_{\mathrm{b}}\hat{\boldsymbol{r}}_{\mathrm{b}}\hat{\boldsymbol{r}}_{\mathrm{b}} & \mathbf{0} & \mathbf{0} \\ \mathbf{0} & \mathbf{0} & \mathbf{0} & \mathbf{0} \\ \mathbf{0} & \mathbf{0} & \mathbf{0} & \mathbf{0} \end{pmatrix}
$$

where $\boldsymbol{r}_{\mathrm{b}} = [r_b, 0, 0]^T$ denotes the location of buoyancy control system with respect to the body frame origin, expressed in the body frame. The kinetic energy of the buoyancy control system is

$$
T_{\mathrm{b}} = \frac{1}{2}\boldsymbol{\eta}^T \mathbb{M}_{\mathrm{b}}\, \boldsymbol{\eta}
$$

Let $\boldsymbol{J}_{\mathrm{rb}}$ denotes the 3×3 matrix of moments and products of inertia for the rigid body, then the generalized mass matrix for the rigid body portion of the glider is

$$
\mathbb{M}_{\mathrm{rb}} = \begin{pmatrix} m_{\mathrm{rb}}\mathbb{I} & -m_{\mathrm{rb}}\hat{\boldsymbol{r}}_{\mathrm{rb}} & \mathbf{0} & \mathbf{0} \\ m_{\mathrm{rb}}\hat{\boldsymbol{r}}_{\mathrm{rb}} & \boldsymbol{J}_{\mathrm{rb}} & \mathbf{0} & \mathbf{0} \\ \mathbf{0} & \mathbf{0} & \mathbf{0} & \mathbf{0} \\ \mathbf{0} & \mathbf{0} & \mathbf{0} & \mathbf{0} \end{pmatrix}
$$

where $\boldsymbol{r}_{\mathrm{rb}} = [0, 0, r_{rb}]^T$ denotes the center of mass position of glider rigid body portion with respect to the body frame origin, expressed in the body frame. The kinetic energy of the rigid body portion is

$$
T_{\mathrm{rb}} = \frac{1}{2}\boldsymbol{\eta}^T \mathbb{M}_{\mathrm{rb}}\, \boldsymbol{\eta}
$$

We finally define the generalized added inertia matrix, which accounts for the energy necessary to accelerate the fluid around the vehicle as it moves:

$$
\mathbb{M}_{\mathrm{f}} = \begin{pmatrix} \boldsymbol{M}_{\mathrm{f}} & \boldsymbol{C}_{\mathrm{f}}^T & \mathbf{0} & \mathbf{0} \\ \boldsymbol{C}_{\mathrm{f}} & \boldsymbol{J}_{\mathrm{f}} & \mathbf{0} & \mathbf{0} \\ \mathbf{0} & \mathbf{0} & \mathbf{0} & \mathbf{0} \\ \mathbf{0} & \mathbf{0} & \mathbf{0} & \mathbf{0} \end{pmatrix}
$$

where the component submatrices $\boldsymbol{M}_{\mathrm{f}}$, $\boldsymbol{J}_{\mathrm{f}}$, and $\boldsymbol{C}_{\mathrm{f}}$ represent added mass, added inertia, and hydrodynamic coupling between the translational and rotational motion of the rigid body[11]. The kinetic energy of the fluid is

$$
T_{\mathrm{f}} = \frac{1}{2}\boldsymbol{\eta}^T \mathbb{M}_{\mathrm{f}}\, \boldsymbol{\eta}
$$

The total kinetic energy of the rigid body/fluid/particle system is

$$
T = T_{\mathrm{p}} + T_{\mathrm{b}} + T_{\mathrm{rb}} + T_{\mathrm{f}} = \frac{1}{2}\boldsymbol{\eta}^T \mathbb{M}(\boldsymbol{r}_{\mathrm{p}})\boldsymbol{\eta}
$$

where

$$
\mathbb{M}(\boldsymbol{r}_{\mathrm{p}}) = \mathbb{M}_{\mathrm{px}}(\boldsymbol{r}_{\mathrm{px}}) + \mathbb{M}_{\mathrm{pxy}}(\boldsymbol{r}_{\mathrm{pxy}}) + \mathbb{M}_{\mathrm{b}} + \mathbb{M}_{\mathrm{rb}} + \mathbb{M}_{\mathrm{f}}
$$

The generalized momentum is

$$
\begin{pmatrix} \boldsymbol{p} \\ \boldsymbol{h} \\ \boldsymbol{p}_{\mathrm{p_x}} \\ \boldsymbol{p}_{\mathrm{p_{xy}}} \end{pmatrix} = \frac{\partial T}{\partial \boldsymbol{\eta}}
$$

where $\boldsymbol{p}$ is the total body translational momentum; $\boldsymbol{h}$ is the total body angular momentum; $\boldsymbol{p}_{\mathrm{p_x}}$ and $\boldsymbol{p}_{\mathrm{p_{xy}}}$ are the moving masses momentum.

The dynamic equations in the body frame are

$$
\dot{\boldsymbol{p}} = \boldsymbol{p}\times\boldsymbol{\omega} + W\boldsymbol{\zeta} + \boldsymbol{f}_{\mathrm{v}} + \boldsymbol{f}_{\mathrm{prop}} \tag{5}
$$

$$
\begin{aligned} \dot{\boldsymbol{h}} = \boldsymbol{h}\times\boldsymbol{\omega} + \boldsymbol{p}\times\boldsymbol{v} + m_{\mathrm{rb}}g\boldsymbol{r}_{\mathrm{rb}}\times\boldsymbol{\zeta} + m_{\mathrm{b}}g\boldsymbol{r}_{\mathrm{b}}\times\boldsymbol{\zeta} \\ + m_{\mathrm{px}}g\boldsymbol{r}_{\mathrm{px}}\times\boldsymbol{\zeta} + m_{\mathrm{pxy}}g\boldsymbol{r}_{\mathrm{pxy}}\times\boldsymbol{\zeta} + \boldsymbol{m}_{\mathrm{v}} + \boldsymbol{m}_{\mathrm{prop}} \end{aligned} \tag{6}
$$

$$
\dot{\boldsymbol{p}}_{\mathrm{p_x}} = \left(\boldsymbol{p}_{\mathrm{px}}\times\boldsymbol{\omega} + m_{\mathrm{px}}g\boldsymbol{\zeta}\right) + u_{\mathrm{p_x}} \tag{7}
$$

$$
\dot{\boldsymbol{p}}_{\mathrm{p_{xy}}} = \left(\boldsymbol{p}_{\mathrm{pxy}}\times\boldsymbol{\omega} + m_{\mathrm{pxy}}g\boldsymbol{\zeta}\right) + u_{\mathrm{p_{xy}}} \tag{8}
$$

where

$$
\boldsymbol{\zeta} = \boldsymbol{R}_{\mathrm{IB}}^T \boldsymbol{i}_3
$$

is the "tilt vector," the body frame unit vector in the direction of gravity; $u_{\mathrm{p_x}}$ is input force from the actuator which adjust the glider's attitude; $\boldsymbol{f}_{\mathrm{v}}$ and $\boldsymbol{m}_{\mathrm{v}}$ represent viscous effects acting on the glider expressed in the body frame; $\boldsymbol{f}_{\mathrm{prop}}$ and $\boldsymbol{m}_{\mathrm{prop}}$ are the force and moment caused by the thruster.

Equations (5) through (8), along with the buoyancy actuator dynamics

$$
\ddot{\mathrm{V}}_b = u_{\mathrm{b}} \tag{9}
$$

describe the hybrid glider dynamics. Here, u_{b} is the input force from the actuator, which adjusts the glider's net weight. Together with the kinematic equations (1) to (4), these equations completely describe the motion of the vehicle in still water. By dynamic model analysis, the model can be used to predict the maneuverability of the hybrid glider. Moreover, the derived dynamic model can be used for control and planning algorithms design next.

IV. THE HYBRID GLIDER PROTOTYPE DESIGN

The hybrid glider is designed to have the horizontal velocity up to 0.9 m/s in AUV mode so that the vehicle can conquer the influence of the current. In normal operation, the vehicle speed is usually 0.3 m/s to 0.5 m/s to reduce drag force so as to achieve long endurance and long range.

As shown in Fig. 2, the hybrid glider can be divided into five sections: Bow Section, Ballast Section, Sensor Section, Main Section, Electronic Section and Thruster Section. Specifically, the Bow Section is a flooded section for the installation of sensors such as USBL transceiver and camera, which are necessary devices for underwater docking; the Ballast Section holds a buoyancy control system which uses a hydraulic pump to transfer oil between an internal reservoir and an external bladder; the Sensor Section is also a flooded section which contains the sensors selected for each mission; the Main Section contains an attitude control system which regulates the pitch and roll angles of vehicle by moving internal masses; the Electronic Section houses the onboard electronics including the main control board, TCM5 Compass, GPS receiver, FreeWave transceiver, etc.; and the Thruster Section includes a thruster which can rotate about its vertical axis, acting as a rudder as well. The specifications for the hybrid glider are presented in Table I. Details of the prototype design are described below.

TABLE I. HYBRID UNDERWATER GLIDER SPECIFICATIONS

Length	2.4 m
Diameter	220 mm
Weight in air	80 kg
Operating Depth	0-200 m
Deflection angle of thruster	±45°
Communications	Freewave Radio; GPS navigation
Battery	Lithium Battery, Energy 2.5 MJ
Operating in glider mode	0.25 m/s ~ 0.4 m/s
Operating in AUV mode	0.3 m/s ~ 0.9 m/s

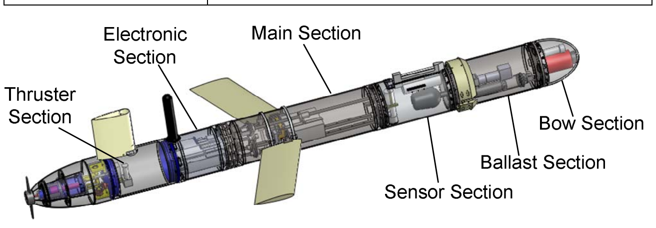

Fig. 2. The hybrid underwater glider

A. *Rotatable Thruster*

The yaw motion of the hybrid glider is controlled by a rotatable thruster which can rotate about its vertical axis. This yields higher maneuverability at low speeds when compared to a traditional fin-maneuver vehicle. The rotatable thruster consists of a thruster and a rotation mechanism.

The thruster is designed to achieve the goals of low power and high efficiency. To this end, the drive chain has to be carefully designed. As shown in Fig. 3, a maxon RE 25 DC motor was chosen as the drive motor, and a gearbox was used to match the speed of the motor to the operational region of the propeller. To achieve high efficiency, the gearbox we chose was the GYSIN planetary gearbox GPL 26. Its efficiency is 90% in the condition of full load. To further reduce the frictional losses due to regular shaft seal, a magnetic coupling was used. The barrier between the inner magnetic hub and the outer magnetic hub was fabricated from titanium alloy TC4 to reduce eddy-current losses.

The rotation mechanism is used to rotate the thruster to control the yaw. It contains a pair of bevel gears, output shaft, swing shaft and a rotation motor. The rotation motor drive the output shaft which passes through the endcap using a rotary shaft seal. The bevel gears are used to transfer the rotation of the output shaft to the rotation of the swing shaft. The bevel gears are made of nylon which resists corrosion in sea water.

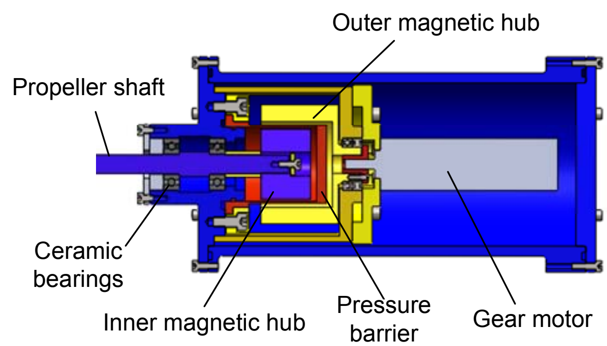

Fig. 3 The structure of the thruster

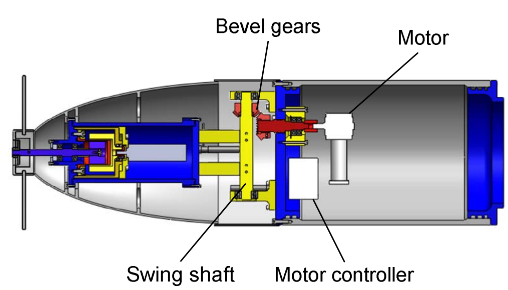

Fig. 4 The rotatable thruster

B. Attitude Control System

The attitude of the hybrid is controlled by two moving masses mechanisms that adjust the vehicle's center of gravity relative to the center of buoyancy. In this design, a single lateral moving mass is driven by a pinion and rack mechanism to regulate the roll angle of the vehicle. Moreover, in AUV mode, the lateral moving mass is used to balance the torque induced by the propeller. The longitudinal moving mechanism is based on a screw-nut assembly. A battery pack together with the lateral moving mass mechanism can be moved along the guide rail to regulate the pitch angle of the vehicle. A worm gearbox is used to reduce the motor speed and provide self-locking mechanism. Two limit switches are mounted on each end of the moving mass's linear travel length. The attitude control system is shown Fig. 5

C. Buoyancy Control System

The buoyancy of the glider is controlled by a hydraulic pump system, which uses a gear pump to transfer oil between an internal reservoir and an external bladder. The internal reservoir is designed as the hydraulic cylinder form, and a pull-wire displacement sensor are used to measure the displacement of cylinder piston, with which the volume of inflated and deflated oil can be measured correctly. More details can be seen in [14].

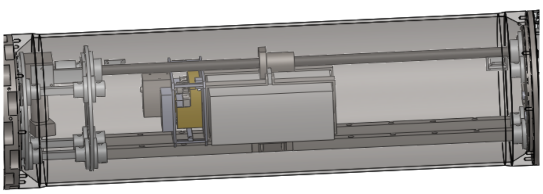

Fig. 5 The attitude control system

D. Electrical Hardware

The control system of the hybrid glider is based on TMS320F28335 digital signal controller, which is highly integrated, high-performance solutions for demanding control applications. Its multiple peripheral ports are very convenient for the integration of other functional devices. These glider function devices include electronic compass, GPS receiver, communication terminal, CTD, depth sensor, altimeter and motor controllers. Fig. 7 shows the control system architecture of the hybrid glider.

E. Other Design Details

The vehicle is designed with modular architecture, which is composed of several sections. To improve the convenience of assembling and maintenance, plug planes between sections are designed (see Fig. 6). The connectors are mounted on the plug planes, and this allows sections to be easily joined or separated.

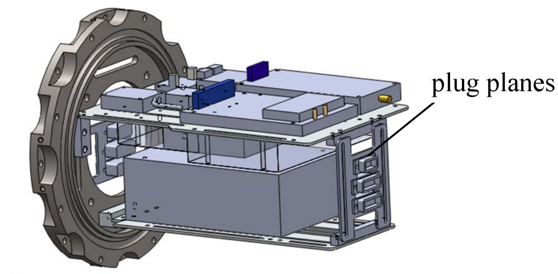

Fig. 6 Plug planes between sections

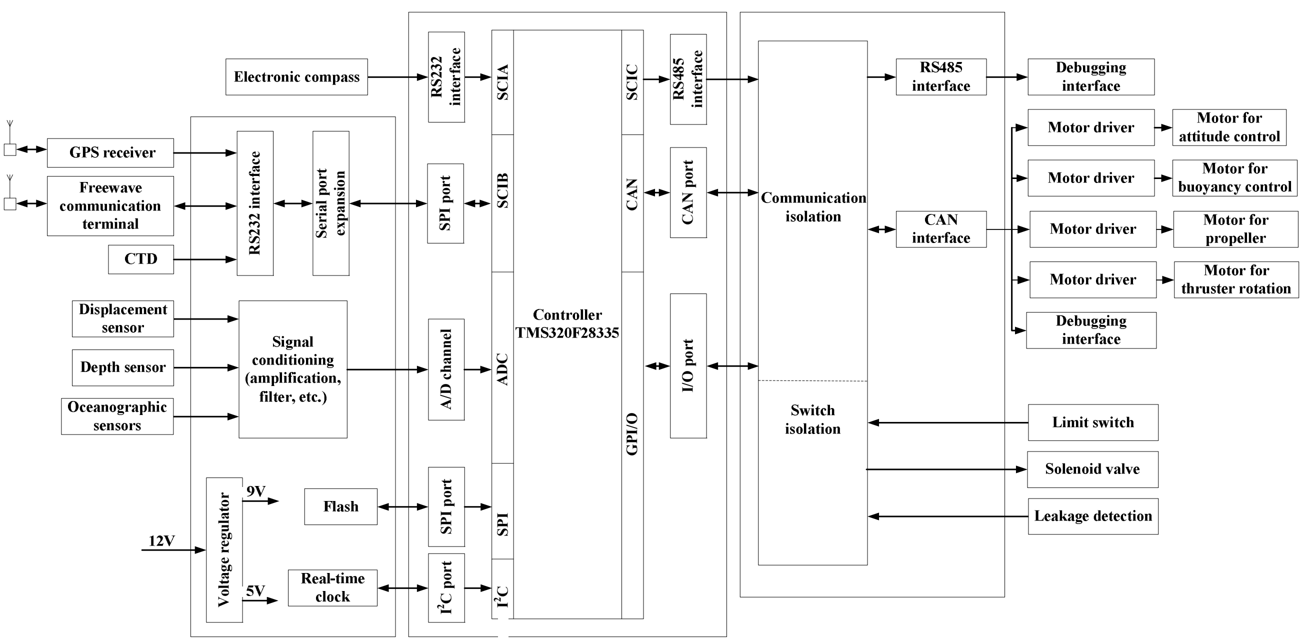

Fig. 7 Control system architecture of the hybrid glider

F. *Components for Docking*

Due to the rotatable thruster design, the vehicle can achieve higher maneuverability even in low advance speed. Owning to its higher maneuverability and its horizontal fly ability, our hybrid glider can dock with an underwater station in propeller-driven AUV mode for battery recharging and data communication. In our design, a USBL transceiver and a camera in the Bow Section are used to provide navigation and vision information in order to guide underwater docking; power transmission and high-speed data communication with the station are achieved by an inductive coil and a radio frequency antenna, respectively. If the docking station is connected to a cabled ocean observatory[15-17], the hybrid gliders can be considered as additional mobile nodes for 3-D ocean observing. This concept is illustrated in Fig. 8. These components for docking are under development.

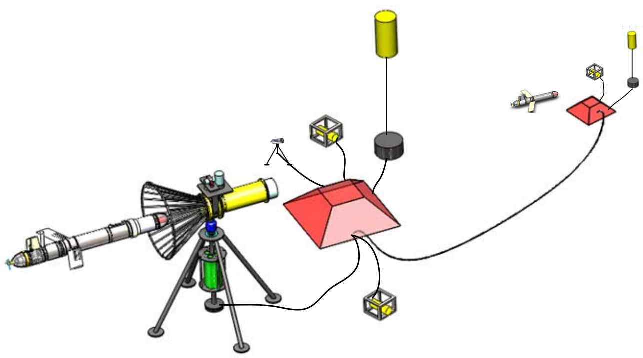

Fig. 8. A hybrid glider docking on a station in the ocean observing system

V. SYSTEM TEST

After the prototype is designed and fabricated, the performance of the individual modules is tested firstly, including the rotation mechanism test and the thruster test. The tests shows that these modules can function as designed. Fig. 9 shows preliminary test of the thruster. Fig. 10 shows the hybrid glider during trimming test. After system trimming, horizontal flight tests and turning tests were conducted in a swimming pool(as shown in Fig. 11). Estimated from the turning tests, the minimum turning radius of the hybrid glider is about 9 m.

Fig. 9 The thruster test

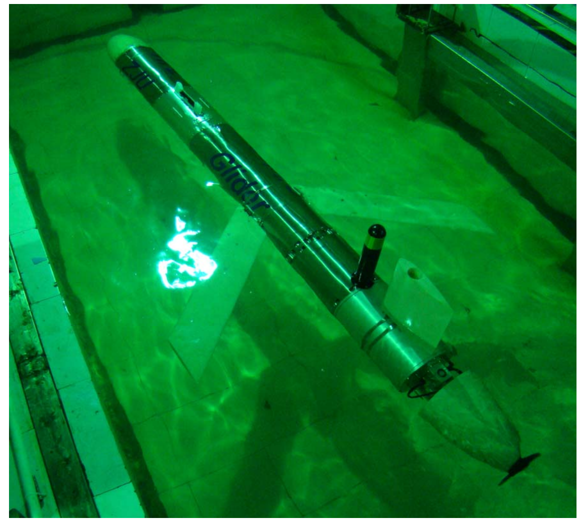

Fig. 10 The hybrid glider trimming test

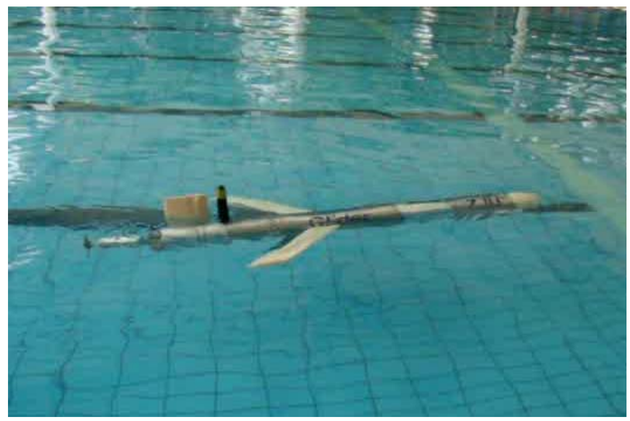

Fig. 11 The hybrid glider in the swimming pool test

VI. CONCLUSIONS

The paper describes the dynamic modeling and design of a hybrid glider for underwater docking. The multi-body dynamic model of the vehicle is first derived. The derived dynamic model can be used to predict the maneuverability of the vehicle and to design the control and planning algorithms next. Then the design of the prototype is presented in detailed. By using a rotatable thruster, the vehicle can achieve high maneuverability in low speed. Owning to its higher maneuverability and its horizontal fly ability, the hybrid glider can dock with an underwater station in propeller-driven AUV mode. Finally, the preliminary tests are introduced. The pool tests show that the hybrid glider can achieve high maneuverability as designed.

Future work includes the pool trials or field trials to further evaluate the performance of the prototype. Components for docking will be developed, and effective control algorithms for underwater docking and the docking tests are the future efforts.

ACKNOWLEDGMENT

The authors are grateful to the State Key Lab of Fluid Power Transmission and Control of Zhejiang University for providing laboratory equipment. In addition, the authors gratefully acknowledge the financial support of the Science Fund for Creative Research Groups of National Natural Science Foundation of China（No.51221004）and the Program for Zhejiang Leading Team of S&T Innovation（Granted No.2010R50036）.

REFERENCES

[1] N. Mahmoudian and C. Woolsey, "Underwater glider motion control,", 2008, pp. 552 -557.

[2] D. L. Rudnick, R. E. Davis, C. C. Eriksen, D. M. Fratantoni, and M. J. Perry, "Underwater gliders for ocean research," MARINE TECHNOLOGY SOCIETY JOURNAL, vol. 38, pp. 73-84, 2004.

[3] B. Claus, R. Bachmayer and C. D. Williams, "Development of an auxiliary propulsion module for an autonomous underwater glider," Proceedings of the Institution of Mechanical Engineers, Part M: Journal of Engineering for the Maritime Environment, vol. 224, pp. 255-266, 2010.

[4] R. Bachmayer, N. E. Leonard, J. Graver, E. Fiorelli, P. Bhatta, and D. Paley, "Underwater gliders: Recent developments and future applications," PROCEEDINGS OF THE 2004 INTERNATIONAL SYMPOSIUM ON UNDERWATER TECHNOLOGY, pp. 195-200, 2004.

[5] "Underwater glider system study, Technical report, Office of Naval Research, U.S.A., 2003,".

[6] A. Alvarez, A. Caffaz, A. Caiti, G. Casalino, L. Gualdesi, A. Turetta, and R. Viviani, "Folaga: A low-cost autonomous underwater vehicle combining glider and AUV capabilities," OCEAN ENGINEERING, vol. 36, pp. 24-38, 2009.

[7] A. Caffaz, A. Caiti, G. Casalino, and A. Turetta, "The Hybrid Glider/AUV Folaga Field Experience at the GLINT'08 Experiment," IEEE ROBOTICS & AUTOMATION MAGAZINE, vol. 17, pp. 31-44, 2010.

[8] S. X. Wang, X. J. Sun, Y. H. Wang, J. G. Wu, and X. M. Wang, "Dynamic Modeling and Motion Simulation for A Winged Hybrid-Driven Underwater Glider," CHINA OCEAN ENGINEERING, vol. 25, pp. 97-112, 2011.

[9] S. X. Wang, X. J. Sun, J. G. Wu, X. M. Wang, and H. W. Zhang, "Motion characteristic analysis of a hybrid-driven underwater glider," in OCEANS'10 IEEE Sydney, OCEANSSYD 2010 Sydney, NSW, Australia, 2010.

[10] Y. Morel, "Design of an adaptive nonlinear controller for an autonomous underwater vehicle equipped with a vectored thruster,": Florida Atlantic University, 2002.

[11] Thor I. Fossen, Guidance and Control of Ocean Vehicles. New York, USA: John Wiley and Sons, Inc, 1995.

[12] N. Mahmoudian, "Efficient Motion Planning and Control for Underwater Gliders,". vol. Doctor of Philosophy: Virginia Polytechnic Institute and State University, 2009.

[13] C. A. Woolsey, "Reduced Hamiltonian dynamics for a rigid body/mass particle system," JOURNAL OF GUIDANCE, CONTROL, AND DYNAMICS, vol. 28, 2005.

[14] S. Fan, C. Yang, S. Peng, K. Li, Y. Xie, and S. Zhang, "Underwater glider design based on dynamic model analysis and prototype development," Journal of Zhejiang University-SCIENCE C, 2013.

[15] Yanhu Chen, Canjun Yang, Dejun Li, Bo Jin, Ying Chen. Design and application of a junction box for cabled ocean observatories system. Marine Technology Society Journal, 2012, 46(3), 50-63.

[16] Yanhu Chen, Canjun Yang, Dejun Li, Bo Jin, Ying Chen. Study of a DC power system for a multi-node cabled ocean observatories system. Journal of Zhejiang University SCIENCE C, 2012, 13(8), 613-623.

[17] Yanhu Chen, Canjun Yang, Dejun Li, Bo Jin, Ying Chen. Study on 10kVDC powered junction box for cabled ocean observatory system. China Ocean Engineering, 2013, 27(2), 265-275